Recent Additions in the Modeling Capabilities for the WEC-Sim-v1.1 Wave Energy Converter Design Tool

Nathan Tom, Michael Lawson, Yi-Hsiang Yu
National Wind Technology Center, National Renewable Energy Laboratory
Golden, Colorado, USA

ABSTRACT

WEC-Sim is a midfidelity numerical tool for modeling wave energy conversion devices. The code uses the MATLAB SimMechanics package to solve multibody dynamics and models wave interactions using hydrodynamic coefficients derived from frequency-domain boundary-element methods. This paper presents the new modeling features introduced in the latest release of WEC-Sim. The first feature discussed is the conversion of the fluid memory kernel to a state-space approximation. This is a substantial computational benefit after the hydrodynamic body-to-body coefficients are introduced and the number of interactions increases exponentially with each additional body. The final features to be introduced is the ability to calculate the wave excitation forces based on the instantaneous incident wave angle allowing the device to weathervane and importation of a user defined wave elevation time series. A review of the hydrodynamic theory for each feature is provided and successful implementation is verified using test cases.

KEY WORDS: Wave energy converter; open source; modeling software.

INTRODUCTION

During the past decade there has been a renewed interest from both the commercial and governmental sectors in the development of marine and hydrokinetic energy. However, wave energy converters (WECs) remain at early stages of development and have not yet proven to be commercially viable. Given the relatively few full-scale device deployments, WEC development is highly dependent on numerical modeling tools to drive innovative designs and advanced control strategies. Conventional seakeeping software has a difficult time modeling new multibody WECs. These complications arise because of the various links between bodies and the additional degrees of freedom required to model the power extraction process.

WEC modeling tools are currently being developed by several companies. These include WaveDyn distributed by Det Norske Veritas – Germanischer Lloyd (DNV-GL) (Mackay, Cruz, Livingstone, and Arnold, 2013), OrcaFlex distributed by Orcina (Orcina, 2014), Aqwa distributed by ANSYS, and INWAVE distributed by INNOSEA (Combourieu, Maxime, Francois, Barbarit, 2014). However, it is desirable to develop open-source modeling tools to establish a collaborative research community that can play a role in accelerating the pace of technology development. To assist the fledgling U.S. marine and hydrokinetic industry, the U.S. Department of Energy (LaBonte, et. al., 2013) has funded a joint initiative between the National Renewable Energy Laboratory (NREL) and Sandia National Laboratories (SNL) to develop a comprehensive wave energy modeling tool to assist both the research and industry communities. The joint effort between NREL and SNL lead to the release of WEC-Sim-v1.0 (Yu, Lawson, Ruehl, Michelen, Tom, 2014) in the summer of 2014. The code was developed in the MATLAB/SIMULINK (MATLAB, 2014) environment using the multibody dynamics solver SimMechanics with preliminary code verification performed in (Ruehl, Michelen, Kanner, Lawson, and Yu, 2014; Yu, Li, Hallet, and Hotimsky, 2014). At the moment, WEC-Sim is best suited to handle rigid multibody dynamics allowing for multiple linkages; however, overtopping and oscillating water column WEC concepts cannot be easily modeled.

This paper provides an overview of the additional modeling capabilities included in WEC-Sim-v1.1 released in March 2015. The first module described is the realization of the fluid memory kernel in state-space form. This ability will help reduce computational time once hydrodynamic body-to-body interactions are introduced. The final hydrodynamic feature described is the weathervaning capability due to the wave excitation force calculation based on the instantaneous incident wave angle. The hydrodynamic theory for each feature is provided before results from test cases are used to verify succesful implementation within WEC-Sim.

STATE-SPACE REPRESENTATION OF THE IMPULSE RESPONSE FUNCTION

In linear water wave theory, the instantaneous wave radiation force, commonly known as the Cummins equation (Cummins, 1962), can be written as:

$$f_r(t) = -\mu_\infty \ddot{\zeta}(t) - \lambda_\infty \dot{\zeta}(t) - \int_{-\infty}^{t} K_r(t-\tau)\dot{\zeta}(\tau)d\tau \quad (1)$$

where μ_∞ is the added mass at infinite frequency, λ_∞ is the wave

damping at infinite frequency, K_r is a causal function known as the radiation impulse-response function, and ζ is the six-degrees-of-freedom vector of body motion. The convolution term in Eq. (1) captures the effect that the changes in momentum of the fluid at a particular time affect the motion at future instances, which can be thought of as a fluid memory effect. The relations between the time- and frequency-domain coefficients were derived in Ogilve (1964) as follows:

$$\lambda(\sigma) = \lambda_\infty + \int_0^\infty K_r(t)\cos\sigma t dt \tag{2}$$

$$\mu(\sigma) = \mu_\infty - \frac{1}{\sigma}\int_0^\infty K_r(t)\sin\sigma t dt \tag{3}$$

where $\mu(\sigma)$ and $\lambda(\sigma)$ are the frequency dependent hydrodynamic radiation coefficients commonly known as the added mass and wave-damping.

The radiation impulse response function can be calculated by taking the inverse Fourier transform of the hydrodynamic radiation coefficients, as found by

$$K_r(t) = -\frac{2}{\pi}\int_0^\infty \sigma\left[\mu(\sigma) - \mu_\infty\right]\sin\sigma t d\sigma \tag{4}$$

$$K_r(t) = \frac{2}{\pi}\int_0^\infty \left[\lambda(\sigma) - \lambda_\infty\right]\cos\sigma t d\sigma \tag{5}$$

where the frequency response of the convolution will be given by

$$\begin{aligned} K_r(j\sigma) &= \int_0^\infty K_r e^{-j\sigma\tau} d\tau \\ &= \left[\lambda(\sigma) - \lambda_\infty\right] + j\sigma\left[\mu(\sigma) - \mu_\infty\right] \end{aligned} \tag{6}$$

Where j is the imaginary unit $\sqrt{-1}$. For most single floating bodies $\lambda_\infty = 0$ and Eq. (5) converges significantly faster than Eq. (4). The hydrodynamic coefficients are solely a function of geometry and the frequency-dependent added mass and wave-damping values can be obtained from boundary element solvers such as WAMIT (Lee, 1995) and NEMOH (Barbarit, 2014).

It is highly desirable to represent the convolution integral shown in Eq. (1) in state-space form (Yu, 1996). This has been shown to dramatically increase computational speeds and allow for conventional control methods, which rely on linear state-space models, to be used. An approximation will need to be made as K_r is obtained from a set of partial differential equations where as a linear state-space model is constructed from a set of ordinary differential equations. In general it is desired to make the following approximation

$$\begin{aligned} &\dot{X}_r(t) = A_r X_r(t) + B_r\dot{\zeta}(t); \quad X_r(0) = 0 \\ &\int_{-\infty}^{t} K_r(t-\tau)d\tau \approx C_r X_r(t) + D_r\dot{\zeta}(t) \end{aligned} \tag{7}$$

where A_r, B_r, C_r, D_r being the time-invariant state, input, output, and feed-through matrices; X_r is the vector of states that describe the convolution kernel as time progresses; and $\dot{\zeta}$ is the input to the system.

The impulse-response of a single-input state-space model represented by:

$$\begin{aligned} \dot{x}(t) &= A_r x(t) + B_r u(t) \\ y(t) &= C_r x(t) \end{aligned} \tag{8}$$

is the same as the unforced response ($u = 0$) with the initial states set to B_r. The impulse response of a continuous system with a nonzero D_r matrix is infinite at $t = 0$, therefore the lower continuity value of $C_r B_r$ is reported at $t = 0$; however, if a D_r matrix results from a given realization method it can be artificially set to 0 with minimal effect on the system response. The general solution to a linear-time invariant system is given by:

$$x(t) = e^{A_r t}x(0) + \int_0^t e^{A_r(t-\tau)}B_r u(\tau)d\tau \tag{9}$$

where e^{A_r} is called the matrix exponential and the calculation of K_r follows:

$$\tilde{K}_r(t) = C_r e^{A_r t}B_r \tag{10}$$

Laplace Transform and Transfer Function

The Laplace transform is a common integral transform in mathematics. It is a linear operator of a function that transforms $f(t)$ to a function $F(s)$ with complex argument, s, which is calculated from the integral:

$$F(s) = \int_0^\infty f(t)e^{-st}dt \tag{11}$$

where the derivative of $f(t)$ has the following Laplace transform:

$$sF(s) = \int_0^\infty \frac{df(t)}{dt}e^{-st}dt \tag{12}$$

Consider a linear input-output system described by the following differential equation

$$\begin{aligned} &\frac{d^m y}{dt^m} + a_1\frac{d^{m-1}y}{dt^{m-1}} + \ldots + a_m y \\ &\qquad = b_o\frac{d^n u}{dt^n} + b_1\frac{d^{n-1}u}{dt^{n-1}} + \ldots + b_n u \end{aligned} \tag{13}$$

where y is the output and u the input. After taking the Laplace transform of Eq. (13), the differential equation is now described by two polynomials

$$\begin{aligned} A(s) &= s^m + a_1 s^{m-1} + \ldots + a_{m-1}s + a_m \\ B(s) &= b_o s^n + b_1 s^{n-1} \ldots + b_{n-1}s + b_n \end{aligned} \tag{14}$$

where $A(s)$ is the characteristic polynomial of the system. The polynomials can be inserted into Eq. (13) leading to:

$$G(s) = \frac{Y(s)}{U(s)} = \frac{s^m + a_1 s^{m-1} + \ldots + a_{m-1}s + a_m}{b_o s^n + b_1 s^{n-1} + \ldots + b_{n-1}s + b_n} \tag{15}$$

where $G(s)$ is the transfer function. If the state input, output, and feed-through matrices are known, the transfer function of the system can be

calculated from

$$G(s) = C_r\left(sI - A_r\right)^{-1} B_r + D_r \tag{16}$$

The frequency response of the system can be obtained by substituting $j\sigma$ for s, over the frequency range of interest, where the magnitude and phase of $G(j\sigma)$ can be calculated with results commonly presented in a Bode plot.

Realization Theory – Frequency Domain

Currently, WEC-Sim allows for the state-space realization of the hydrodynamic radiation coefficients either in the frequency- (FD) or time-domain (TD); however, the frequency domain realization requires the Signal Processing Toolbox distributed by MATLAB. In this analysis the frequency response, $K_r(j\sigma)$, of the impulse-response function is used to best fit a rational transfer function $G(s)$, which is then converted to a state-space model. The general form of a single-input, single-output transfer function of order n and relative degree n-m is given by

$$G(s,\gamma) = \frac{A(s,\gamma)}{B(s,\gamma)} = \frac{s^m + a_1 s^{m-1} + \ldots + a_m}{b_0 s^n + b_1 s^{n-1} + \ldots + b_n} \tag{17}$$

$$\gamma = \left[a_1, \ldots, a_m, b_0, \ldots, b_n\right]^T \tag{18}$$

WEC-Sim utilizes a nonlinear least-squares solver to estimate the parameters of γ. The estimation can only be made after the order and relative degree of $G(s)$ are decided, at which point the following least-squares minimization can be performed

$$\gamma^* = \arg\min_{\gamma} \sum_i w_i \left| K_r\left(j\sigma\right) - \frac{A(j\sigma)}{B(j\sigma)} \right|^2 \tag{19}$$

where w_i is an individual weighting value for each frequency. An alternative that linearizes Eq. (19), proposed by Taghipour, Perez, and Moan (2008), requires the weights to be chosen as

$$w_i = \left|B\left(j\sigma,\gamma\right)\right|^2 \tag{20}$$

which reduces the problem to

$$\gamma^* = \arg\min_{\gamma} \sum \left|B\left(j\sigma,\gamma\right)K_r\left(j\sigma\right) - A\left(j\sigma,\gamma\right)\right|^2 \tag{21}$$

However, depending on the data to be fitted the transfer function may be unstable, because stability is not a constraint used in the minimization. If this occurs, the unstable poles are reflected about the imaginary axis. The relative order of the transfer function can be determined from the initial value theorem

$$\lim_{t\to 0} K_r(t) = \lim_{s\to\infty} sK_r(s) = \lim_{s\to\infty} s\frac{A(s)}{B(s)} = \frac{s^{m+1}}{b_0 s^n} \tag{22}$$

For the above limit to be finite and nonzero the relative order of the transfer function must be one ($n = m + 1$).

Realization Theory – Time Domain

This methodology consists of finding the minimal order of the system and the discrete time state matrices (A_d, B_d, C_d, D_d) from samples of the impulse-response function. This problem is easier to handle for a discrete-time system, because the impulse-response function is given by the Markov parameters of the system

$$\tilde{K}_r(t_k) = C_d A_d^k B_d \tag{23}$$

where $t_k = k\Delta t$ for k = 0,1,2, … and Δt is the sampling period. The above equation does not include the feed-through matrix as it results in an infinite value at $t=0$ and is removed to keep the causality of the system.

The most common algorithm to obtain the realization is to perform a singular value decomposition (SVD) on the Hankel matrix of the impulse-response function as proposed in Kung (1978). The order of the system and corresponding state-space parameters are determined from the number of significant Hankel singular values. Performing an SVD produces:

$$H = \begin{bmatrix} K_r(2) & K_r(3) & \cdots & K_r(n) \\ K_r(3) & K_r(4) & \cdots & 0 \\ \vdots & \vdots & \ddots & \vdots \\ K_r(n) & 0 & \cdots & 0 \end{bmatrix} \tag{24}$$

$$H = U\Sigma V^* \tag{25}$$

where H is the Hankel matrix, and Σ is a diagonal matrix containing the Hankel singular values in descending order. Examination of the Hankel singular values reveals there are generally only a small number of significant states, and model reduction can be performed without a significant loss in accuracy (Taghipour, Perez, and Moan, 2008; Kristiansen, Hijulstad, and Egeland, 2005). Further detail about the SVD method and calculation of the state-space parameters will not be discussed in this paper, and the reader is referred to (Kung, 1978; Taghipour, Perez, and Moan, 2008; Kristiansen, Hijulstad, and Egeland, 2005).

Quality of Realization

WEC-Sim evaluates the quality of the resulting state-space model via the frequency response when using the frequency-domain realization and the corresponding impulse-response for the time-domain realization. To evaluate these responses the coefficient of determination, R^2, is computed according to

$$R^2 = 1 - \frac{\sum\left(K_r - \tilde{K}_r\right)^2}{\sum\left(K_r - \overline{K}_r\right)^2} \tag{26}$$

where $\tilde{K}_r$ represents the resulting hydrodynamic values from the state-space model and $\overline{K}_r$ is the mean value of the reference (true) values. The summations are performed across all frequencies to provide a measure of the variability of the function that is captured by the model.

Application of state-space realization

A truncated vertical cylindrical floater has been chosen as the sample geometry to compare the frequency- and time-domain realizations. The

floater geometric parameters and tank dimensions are found in Table 1 and the hydrodynamic radiation coefficients were calculated from Yeung (1981). The hydrodynamic coefficients were obtained between 0.05 rad/s and − 11 rad/s at 0.05 rad spacing.

In this example, an R^2 threshold of 0.99 was set and the resulting realizations for the impulse-response function and the frequency-dependent radiation coefficients are found in Fig. 1 and Fig. 2. In this example the time-domain characterization outperforms the frequency-domain regression, and the major difference appears in the wave-damping estimation. It was found that the time-domain characterization had better stability than the frequency-domain regression, because it does not require reflection of the unstable poles about the imaginary axis. WEC-Sim users should check the quality of the hydrodynamic data with the custom WEC-Sim MATLAB functions that perform the realizations without running full simulations. These codes allow users to set various fitting parameters using an iterative interface that plots how the fit changes with increasing state-space order. The user can fine tune the input parameters in WEC-Sim so the desired performance is achieved.

Table 1. Floater geometric parameters and tank dimensions.

D (diameter) = 2 a = 0.273 m	d (draft) = 0.613 m	h (tank depth) = 1.46 m

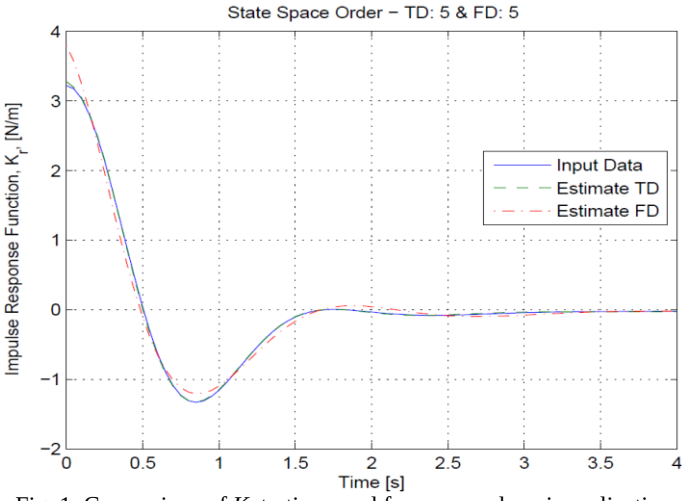

Fig. 1. Comparison of K_r to time- and frequency- domain realizations

HYDRODYNAMIC CROSS COUPLING FORCES

For a single floating body, the time-domain representation of the radiation forces is given by Eq. 1, because it is dependent only on its own motion. However, most WECs consist of multiple floating bodies that can be in very close proximity, and as a result additional interaction forces arise. These forces are generated as the motion of nearby floating bodies alters the local wave field. Unique to floating-body hydrodynamics are the forces felt by one body because of the motion of "n" additional bodies. This is reflected in the off diagonal terms of the added mass and wave-damping matrices which generate a force on Body 1 because of the acceleration and velocity of bodies 2 through n. Because of the reciprocity relationship (Newman, 1977), a consequence of applying Green's Second Identity, the cross diagonal hydrodynamic coefficients are equal

$$\mu_{ij} + \frac{\lambda_{ij}}{-j\sigma} = \mu_{ji} + \frac{\lambda_{ji}}{-j\sigma} \tag{27}$$

Thus a symmetry check can be performed on the numerical values obtained from boundary element solvers such as WAMIT and NEMOH.

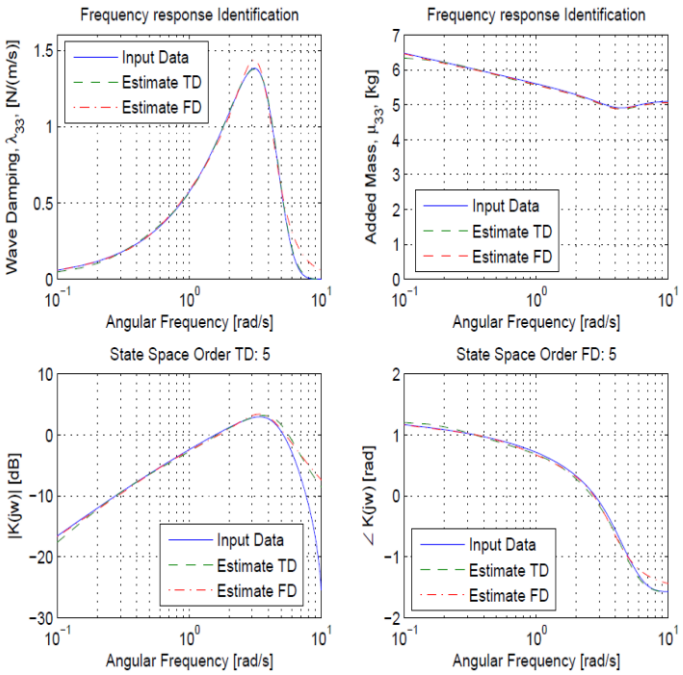

Fig. 2. Frequency response of time- & frequency-domain realizations

Response Amplitude Operator (RAO)

It is common practice to calculate the response amplitude operator to access the performance of a WEC. For an incident wave of amplitude A and frequency σ the response of the floating body is given by ζ_i:

$$\eta(x,t) = \Re\left\{Ae^{j(\sigma t - kx)}\right\} \tag{28}$$

$$\zeta_i(t) = \Re\left\{\xi_i e^{j\sigma t}\right\} \tag{29}$$

where k is the wave number and ξ_i is the complex amplitude of motion for the i-th direction. The resulting harmonic motion, when allowing six degrees of freedom for all floating bodies, can be described by the following coupled system of differential equations:

$$\sum_{k=1}^{6\times n}\left[C_{ik} - \sigma^2\left(I_{ik} + \mathbf{M}_{ik}\right) + j\sigma\Lambda_{ik}\right]\xi_k = F_i \tag{30}$$

where I_{ik} is the generalized inertia matrix for all floating bodies, Λ_{ik} is the generalized wave damping matrix, M_{ik} is the generalized added mass matrix, C_{ik} is the restoring matrix, and F_i is the complex amplitude of the wave-exciting force for all floating bodies. The full description of the matrices can be found in (Newman, 1977) or another introductory hydrodynamic textbook.

Validation of a Generic 5 Body WEC

A generic set of five identical point absorbers were chosen to validate WEC-Sim's ability to handle multibody interactions. For demonstration purposes all bodies will be constrained to heave allowing one to simplify Eq. (30), though extending the equation of motion to consider additional degrees of freedom is easily achieved.

The Simulink model constructed for this task can be seen in Fig. 3.

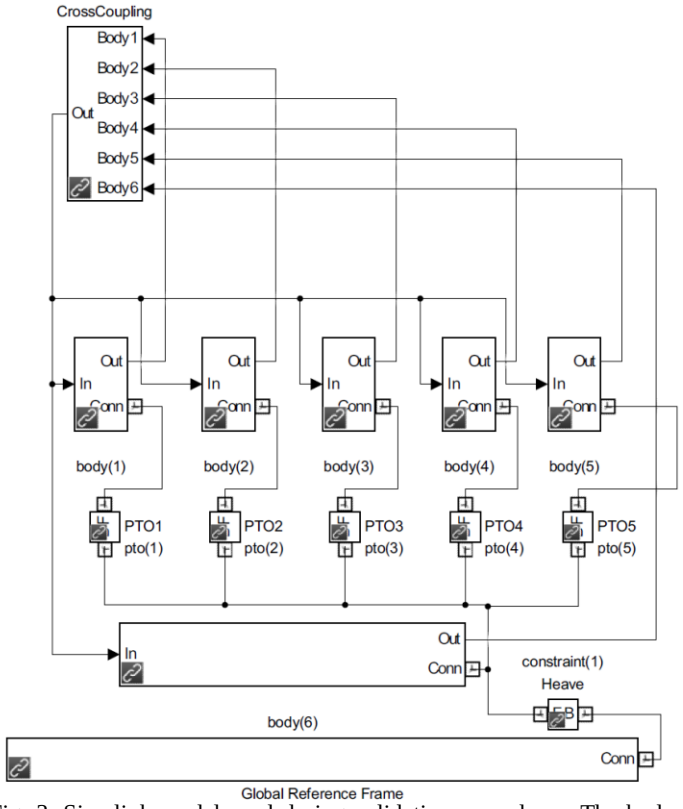

Fig. 3. Simulink model used during validation procedure. The body, constraint, pto, and cross coupling blocks are custom built and appear in the Simulink library.

Inclusion of Linear Power-Take-Off System

In order to extract any power from the incident waves a power-take-off (PTO) system is required, predominantly either a hydraulic or electrical generator. The most generic form for the PTO reaction force is given by

$$f_{PTO} = -C_g \zeta_{rel} - B_g \dot{\zeta}_{rel} - \mu_g \ddot{\zeta}_{rel} \tag{31}$$

where ζ_{rel} is the relative motion between the floating bodies of which the PTO is attached. However, for this test case each point absorber is attached to a fixed submerged body. Thus, the relative velocity will reduce to the velocity of each body. The generator spring, damping, and inertia force coefficients are given by C_g, B_g, and μ_g, respectively. In the frequency domain, adding the PTO force contribution to Eq. (30), while ignoring C_g and μ_g gives

$$\begin{aligned}
&\underbrace{\left\{C_{33} - \sigma^2\left(m_1 + \mu_{33}\right)\right\} + j\sigma\left[\lambda_{33} + B_g\right]}_{a_1}\xi_3 \\
&+\underbrace{\left[-\sigma^2\mu_{39} + j\sigma\lambda_{39}\right]}_{b_1}\xi_9 + \underbrace{\left[-\sigma^2\mu_{315} + j\sigma\lambda_{315}\right]}_{c_1}\xi_{15} \\
&+\underbrace{\left[-\sigma^2\mu_{321} + j\sigma\lambda_{321}\right]}_{d_1}\xi_{21} + \underbrace{\left[-\sigma^2\mu_{327} + j\sigma\lambda_{327}\right]}_{e_1}\xi_{27} = AX_3
\end{aligned} \tag{32}$$

$$\begin{aligned}
&\underbrace{\left[-\sigma^2\mu_{93} + j\sigma\lambda_{93}\right]}_{a_2}\xi_3 + \underbrace{\left\{C_{99} - \sigma^2\left(m_2 + \mu_{99}\right)\right\} + j\sigma\left[\lambda_{99} + B_g\right]}_{b_2}\xi_9 \\
&+\underbrace{\left[-\sigma^2\mu_{915} + j\sigma\lambda_{915}\right]}_{c_2}\xi_{15} + \underbrace{\left[-\sigma^2\mu_{921} + j\sigma\lambda_{921}\right]}_{d_2}\xi_{21} \\
&+\underbrace{\left[-\sigma^2\mu_{927} + j\sigma\lambda_{927}\right]}_{e_2}\xi_{27} = AX_9
\end{aligned} \tag{33}$$

where X_i is the wave-exciting force per unit amplitude wave. Subscripts 3 and 9 denote the first two bodies and three additional equations are necessary to complete the entire system. The above system of equations can be solved to obtain the complex amplitudes of motion (ξ_3, ξ_9, ξ_{15}, ξ_{21}, ξ_{27}) from basic matrix algebra:

$$\begin{bmatrix} \xi_3/A \\ \xi_9/A \\ \xi_{15}/A \\ \xi_{21}/A \\ \xi_{27}/A \end{bmatrix} = \begin{bmatrix} a_1 & b_1 & c_1 & d_1 & e_1 \\ a_2 & b_2 & c_2 & d_2 & e_2 \\ a_3 & b_3 & c_3 & d_3 & e_3 \\ a_4 & b_4 & c_4 & d_4 & e_4 \\ a_5 & b_5 & c_5 & d_5 & e_5 \end{bmatrix}^{-1} \begin{bmatrix} X_3 \\ X_9 \\ X_{15} \\ X_{21} \\ X_{27} \end{bmatrix} \tag{34}$$

The results provide theoretical values to verify WEC-Sim ensuring proper implementation.

The time-domain corollary of Eqs. (32) and (33) is given by the following coupled equations of motion

$$\begin{aligned}
&\left(m_1 + \mu_{33}(\infty)\right)\ddot{\zeta}_3(t) + \mu_{39}(\infty)\ddot{\zeta}_9(t) + \mu_{315}(\infty)\ddot{\zeta}_{15}(t) + \mu_{321}(\infty)\ddot{\zeta}_{21}(t) \\
&+ \mu_{327}(\infty)\ddot{\zeta}_{27}(t) + \int_{-\infty}^{t} K_{r33}(t-\tau)\dot{\zeta}_3(\tau)d\tau + \int_{-\infty}^{t} K_{r39}(t-\tau)\dot{\zeta}_9(\tau)d\tau \\
&+ \int_{-\infty}^{t} K_{r315}(t-\tau)\dot{\zeta}_{15}(\tau)d\tau + \int_{-\infty}^{t} K_{r321}(t-\tau)\dot{\zeta}_{21}(\tau)d\tau \\
&+ \int_{-\infty}^{t} K_{r327}(t-\tau)\dot{\zeta}_{27}(\tau)d\tau + B_g\dot{\zeta}_3(t) + C_{33}\zeta_3(t) = f_{e3}(t)
\end{aligned} \tag{35}$$

$$\begin{aligned}
&\mu_{93}(\infty)\ddot{\zeta}_3(t) + \left(m_2 + \mu_{39}(\infty)\right)\ddot{\zeta}_9(t) + \mu_{915}(\infty)\ddot{\zeta}_{15}(t) + \mu_{921}(\infty)\ddot{\zeta}_{21}(t) \\
&+ \mu_{921}(\infty)\ddot{\zeta}_{21}(t) + \int_{-\infty}^{t} K_{r93}(t-\tau)\dot{\zeta}_3(\tau)d\tau + \int_{-\infty}^{t} K_{r99}(t-\tau)\dot{\zeta}_9(\tau)d\tau \\
&+ \int_{-\infty}^{t} K_{r915}(t-\tau)\dot{\zeta}_{15}(\tau)d\tau + \int_{-\infty}^{t} K_{r921}(t-\tau)\dot{\zeta}_{21}(\tau)d\tau \\
&+ \int_{-\infty}^{t} K_{r921}(t-\tau)\dot{\zeta}_{21}(\tau)d\tau + B_g\dot{\zeta}_9(t) + C_{99}\zeta_9(t) = f_{e9}(t)
\end{aligned} \tag{36}$$

These are implemented in WEC-Sim for the first two bodies. These are the general form for each of the other three bodies and it can be seen that five convolution integrals need to be solved per each equation. Without use of the state-space approximation the computational time increases dramatically with each interacting body especially if other modes of motion, such as surge and pitch, are included.

The comparisons of the frequency-domain to the time-domain solution are provided in Fig. 4 - Fig. 6. The magnitude of the heave response amplitude operator, Fig. 4, shows very good agreement between the frequency- and time-domain solutions with very little variation between bodies. The summation of the RAOs across all bodies, Fig. 5, also shows very good agreement and provides a metric to indicate that the power absorption is relatively equal between both methods. The phase of the RAO provided in Fig. 6, has a significant amount of oscillations for the outer bodies in the high frequency regime

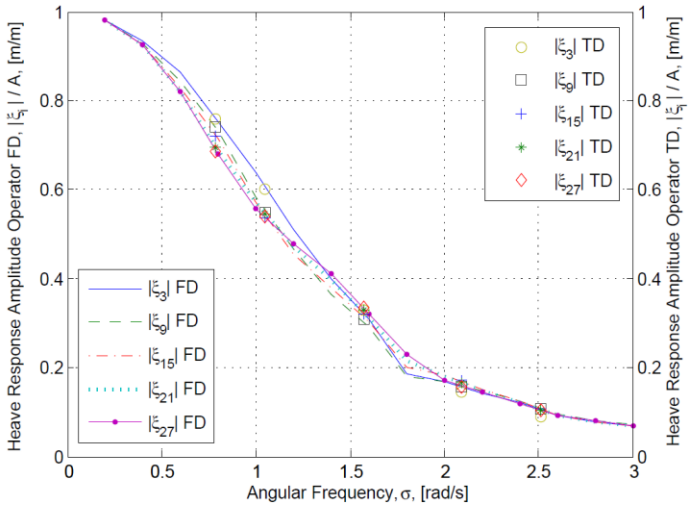

Fig. 4. Comparison between the frequency- and time-domain calculations of the coupled heave motion with B_g = 300 kN/(m/s).

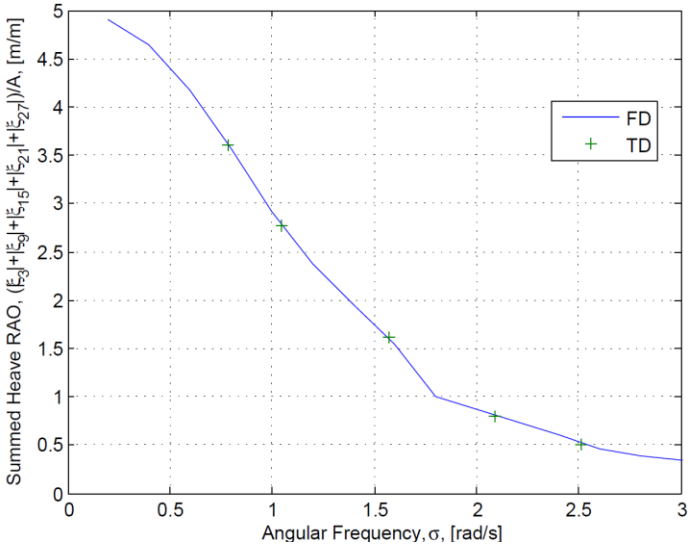

Fig. 5. Comparison of the summed heave motion of the five floating bodies between the frequency- and time-domain coupled calculations.

yet WEC-Sim is still capable of capturing these effects. A comparison between the uncoupled and coupled equations of motion can be found in Fig. 7, which shows that when neglecting coupling effects the absorbed power can be reduced by up to 20 percent in the most energetic states.

WAVE DIRECTIONALITY, WEATHERVANING, and USER DEFINED WAVE ELEVATION

One issue that arises in the design of WECs is the performance sensitivity with respect to the wave heading. It can be shown that an asymmetric wave energy converter can have an extraction efficiency up to unity (Madhi, Sinclair, Yeung, 2013) but the device must be perpendicular to the oncoming wave crest. This may be an appropriate assumption if the device is deployed near shore; however in deep water the device will be subjected to oblique waves likely leading to performance degradation. Furthermore, WECs deployed in deep water will generally rely on mooring lines to provide rotational stiffness thereby allowing the body to yaw where performance can again suffer. Therefore, it is important to have the modeling tools available to allow the WEC to weathervane.

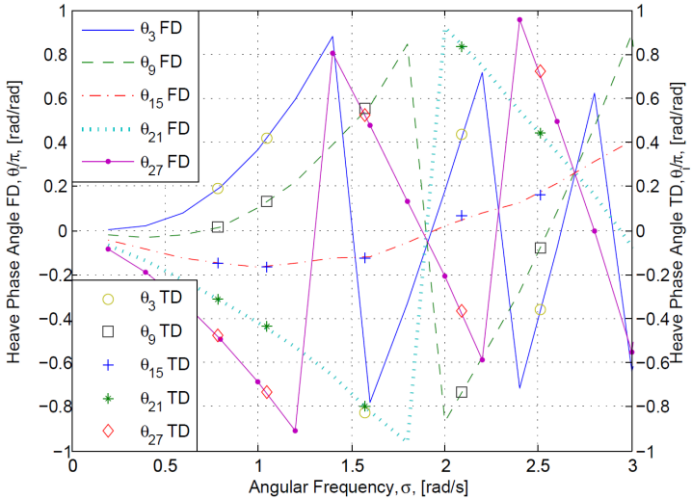

Fig. 6. Comparison of the coupled phase of the five floating bodies between the frequency- and time-domain calculations.

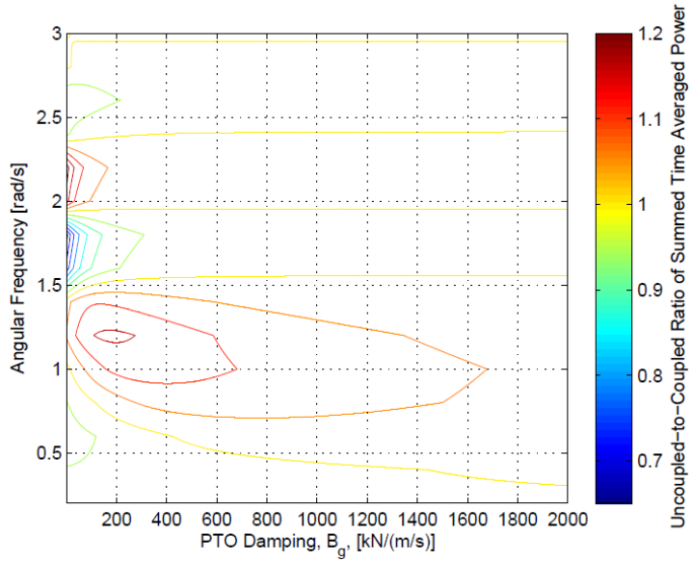

Fig. 7. Ratio of the uncoupled-to-coupled time averaged power.

The incident wave potential, ϕ_I, when accounting for a variable wave heading, is given by:

$$\phi_I(x,y,z,t) = \Re\left\{\frac{jgA}{\sigma}\frac{\cosh k(z+h)}{\cosh kh}e^{j(\sigma t - k(x\cos\beta + y\sin\beta))}\right\} \qquad (37)$$

where g is the gravitational acceleration, A is the wave amplitude, k is the wave number, h is the water depth, and β is the wave heading measured counter clockwise from the positive x-axis.

As the wave heading rotates the only hydrodynamic coefficients that will change are the exciting forces as the radiation forces are strictly body motion dependent. Most boundary element methods can be set to output the wave exciting forces for a given number of incident wave angles. However, when the body is free to rotate the incident wave angle becomes the difference between the wave heading and the yaw angle of the body. Following WAMIT® notion, β ranges from 0 – 360 degrees and a 2π correction must be made if the yaw angle exceeds the wave heading as follows

$$\alpha = \begin{cases} \beta - \xi_6 & \text{if } \xi_6 < \beta \\ 2\pi + \beta - \xi_6 & \text{if } \xi_6 > \beta \end{cases} \tag{38}$$

where α is the incident wave angle and ξ_6 is the yaw angle of the body measured counter clockwise from the positive x-axis.

For demonstration purposes a horizontal half cylinder with a radius, r, of 1 m and a length, L, of 10 m was chosen as the frontal area changes with wave heading. The half cylinder is assumed to have a uniform density equal to the fluid density.

The half cylinder was initial set along the y-axis and was impinged upon by a regular wave with a heading of 22.5 degrees, amplitude of 1 m, and period, T, of 10 s. A wave ramp duration equal to five times the wave period was implemented in order to reduce any impulse effects. The body motion was restricted only to yaw and no external springs were included for yaw stiffness. The results from the simulation can be seen in Fig. 8 and Fig. 9 which plot the body yaw and wave exciting force time history, respectively. As the dynamic model is linear the yaw time history exhibits the typical response of damped second order system with a constant set point. The body yaws from its initial position overshooting the wave heading before dropping into a decaying oscillation. The overshoot is due to the system being underdamped despite the addition of a nonlinear drag term. As seen in Fig. 9, the yaw wave exciting force drops to zero as the yaw angle crosses the heading with smaller oscillations associated with the wave period. In this sense the exciting force acts as a restoring coefficient based on the difference between yaw angle and wave heading.

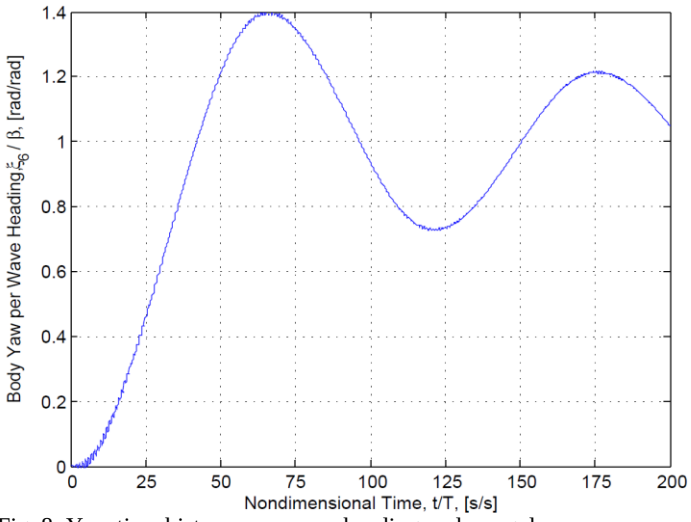

Fig. 8: Yaw time history over wave heading under regular waves.

Often during tank or sea trials, custom time series are measured and can now be imported into WEC-Sim for validation purposes. In order for the user to import a custom wave time series the excitation force kernel must be constructed. The wave exciting force time series is then obtained by convolving the excitation force kernel with the wave elevation as follows

$$f_{ei}(t) = \int_{-\infty}^{\infty} K_{e_i}(t-\tau)\eta(0,\tau)d\tau \tag{39}$$

The excitation force kernel is calculated by taking the inverse Fourier transform of the frequency dependent wave exciting force coefficients

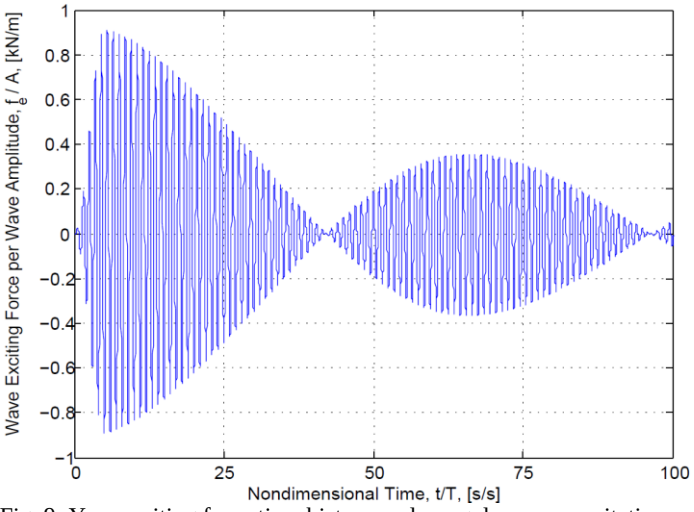

Fig. 9: Yaw exciting force time history under regular wave excitation.

$$K_{e_i}(t) = \frac{1}{2\pi}\Re\left\{\int_{-\infty}^{\infty} X_i(\sigma)e^{j\sigma t}d\sigma\right\} \tag{40}$$

Since K_e is real the following identity can be used, $X_i(-\sigma) = X_i^*(\sigma)$, where * is this case denotes the complex conjugate. This simplifies Eq. (41) to

$$K_{e_i}(t) = \frac{1}{\pi}\int_0^{\infty} \left[\Re\{X_i(\sigma)\}\cos\sigma t - \Im\{X_i(\sigma)\}\sin\sigma t\right]d\sigma \tag{41}$$

where $\Re$ and $\Im$ denote the real and imaginary components, respectively. The half cylinder surge exciting force kernel is plotted in Fig. 10, which is noncausal because of the time history before t = 0. The high frequency oscillations are a result of low resolution of X_1 in the high frequency regime; however, the oscillations are outside of typical wave frequencies and are filtered out after the convolution. Equation (40) produces the same surge exciting force when compared to linear superposition theory verifying proper implementation within WEC-Sim.

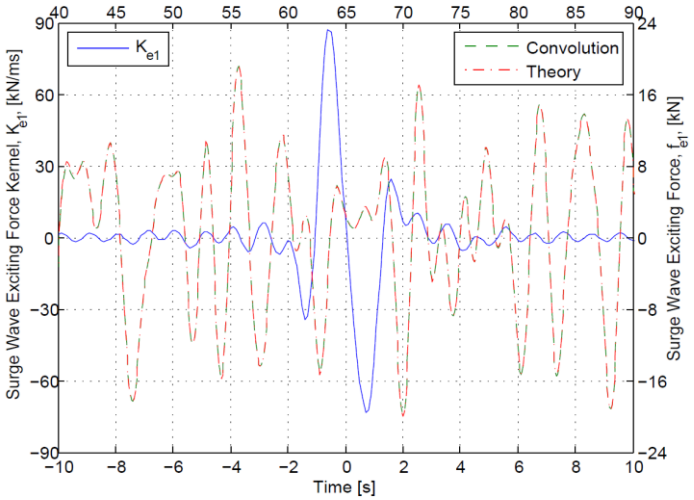

Fig. 10: Surge exciting force kernel for the half cylinder and an irregular surge wave exciting force time history that compares the convolution calculation to the traditional linear superposition theory.

CONCLUSIONS

The work presented in this paper highlights several of the new modeling capabilities included in the latest WEC-Sim-v1.1 release. This includes conversion of the fluid memory kernel to state-space form. Simulations showed that over the operating range of frequencies the state-space representation was able to adequately reproduce the hydrodynamic radiation coefficients; however, a relatively high R^2 may need to be set. Because many wave energy converters consist of two or more excited bodies the ability to model the body-to-body hydrodynamics were added to WEC-Sim. This is an important feature to consider during the design process as the effects can lead to reduced floater motion thereby decreasing annual energy production. Combined with the state space representation significant reductions in computational time were observed compared to the default convolution integral calculation. Finally, the hydrodynamic theory allowing a WEC to weathervane and account for wave directionality was presented. Implementation was performed by interpolation of the excitation forces based on the instantaneous incident wave heading. This capability was included as WECs deployed in the open ocean at times will be subject to oblique waves where the resulting motions and power performance must be evaluated. Furthermore, the theory to calculate the wave excitation force from a user defined wave elevation was provided. The test case showed the convolution method provided accurate forces, when compared to traditional frequency based methods, which allows custom time series measured during tank tests to be used for validation purposes

The release of WEC-Sim-v1.1 also includes a module to calculate the instantaneous nonlinear hydrostatic and hydrodynamic forces as described in (Lawson, Yu, Nelessen, Ruehl, Michelen, 2014). Furthermore, WEC-Sim now boasts the ability to handle Morison elements. However, the fluid particle velocity is calculated assuming the incident wave potential passes undisturbed through the WEC device which is physically unrealistic, but highlights the limitations with mid-fidelity codes. Calculation of the instantaneous fluid velocity and local wave field would require the use of high fidelity numerical codes resulting in large increases in computational time and unnecessary for preliminary design iterations. The modeling capabilities of WEC-Sim-v1.1 have significantly increased and is now more competitive with other code developers. Though WEC-Sim was constructed to assist developers with limited hydrodynamic backgrounds as model complexities increase the user must take additional care in the quality of the hydrodynamic characterization since model performance becomes more sensitive to the given inputs.

ACKNOWLEDGEMENTS

The authors would like to acknowledge the assistance provided by Kelley Ruehl and Carlos Michelen from Sandia National Laboratories for their assistance in the development of the WEC-Sim and the version 1.1 release. This work was supported by the U.S. Department of Energy under Contract No. DE-AC36-083GO28308 with the National Renewable Energy Laboratory. Funding for the work was provided by the DOE Office of Energy Efficiency and Renewable Energy, Wind and Water Power Technologies Office.

REFERENCES

Babarit, A (2014) *NEMOH*, Laboratory for Research in Hydrodynamics, Energy, Environment, and Atmosphere, http://lheea.ec-nantes.fr/doku.php/ emo/nemoh/start?&#nemoh.

Combourieu, A, Maxime, P, Francois, R., and Barbarit, A (2014). "INWAVE: A New Flexible Design Tool Dedicated to Wave Energy Converters," *Proc. 33rd Intl. Conf. on Ocean, Offshore, and Artic Eng.*, San Francisco, CA, USA.

Cummins, WE (1962). "The Impulse Response Function and Ship Motions," *Schiffstechnik*, 9(101).

LaBonte, A, White, B, Lawson, M, Yu, Y-H, Ruehl, K, Bull, D, Li, Y, Thresher, R, Laird, D (2013). "Wave Energy Converter Simulation: Development, Code Competition, and Validation Efforts," *Proc. 10th European Wave and Tidal Energy Conf.*, Aalborg, Denmark, 15.

Kristiansen, E, Hijulstad, A, and Egeland, O (2005). "State-space Representation of Radiation Forces in Time-domainn Vessel Models," *Ocean Eng.*, 32(17−18), 2195−2216.

Kung, SY (1978). "A New Identification and Model Reduction Algorithm via Singular Value Decompositions," *12th IEEE Asilomar Conf. on Circuits, Systems and Computers*," Pacific Grove, CA, USA, 705−714.

Lawson, MJ, Yu, Y-H, Nelessen, A, Ruehl, K, and Michelen, C (2014). "Implementing Nonlinear Buoyancy and Excitation Forces in the WEC-SIM Wave Energy Converter Modeling Tool," *Proc. 33rd Intl. Conf. on Ocean, Offshore, and Artic Eng.*, San Francisco, CA, USA.

Lee, CH (1995). *WAMIT Theory Manual*. Massachusetts Institue of Technology.

Mackay, E, Cruz, J, Livingstone, MJ, and Arnold, P (2013). "Validation of a Time-Domain Modelling Tool for Wave Energy Converter Arrays," *Proc. 10th European Wave and Tidal Energy Conf.*, Aalborg, Denmark, 12.

Madhi, F, Sinclair, ME, and Yeung, RW (2013). "The "Berkeley Wedge": an Asymmetrical Energy-capturing Floating Breakwater of High Performance," *Marine Sys. Ocean Tech.*, 9(1), 5−16.

MATLAB Release 2014a, The MathWorks, Inc. (2014). Natick, Massachusetts, United States. Retrieved from http://www.mathworks.com/products/matlab.

Neary, V, Previsic, M, Jepsen, RA, Lawson, MJ, Yu, Y-H, Copping, AE, et al. (2014). *Methodology for Design and Economic Analysis of Marine Energy Conversion (MEC) Technologies*, Albuquerque, NM, USA, Sandia National Laboratories, SAND2014-9040-RMP.

Newman, JH (1977). *Marine Hydrodynamics*. Massachusetts Institiue of Technology Press, Cambridge, MA.

Ogilvie, T (1964) "Recent Progress Towards the Understading and Prediction of Ship Motions," *Proc. 5th Symp. Naval Hydrodynamics*, Washington, D.C., USA, 3-128.

Orcina, Ltd (2014). *OrcaFlex Manual, Version 9.7a.*

Ruehl, K, Michelen, C, Kanner, S, Lawson, M, and Yu, Y-H (2014). "Preliminary Verification and Validation of WEC-Sim, an Open-Source Wave Energy Converter Design Tool," *Proc. 33rd Intl. Conf. on Ocean, Offshore, and Artic Eng.*, San Francisco, CA, USA.

Taghipour, E, Perez, T, and Moan, T (2008). "Hybrid Frequency-time Domain Models for Dynamic Response Analysis of Marine Structures," *Ocean Eng.*, 35(7), 685−705.

Yeung, RW (1981). "Added Mass and Damping of a Vertical Cylinder in Finite-depth Waters," *Appl. Ocean. Res.*, 3(3), 119−133.

Yu, Y-H, Lawson, MJ, Ruehl, K, Michelen, C, and Tom, N (2014). *WEC-Sim on OPENEI*, http://en.openei.org /wiki/WEC-Sim.

Yu, Y-H, Li, Y, Hallet, K, and Hotimsky, C (2014). "Design and Analysis for a Floating Oscillating Surge Wave Energy Converter," *Proc. 33rd Intl. Conf. on Ocean, Offshore, and Artic Eng.*, San Francisco, CA, USA.

Yu, Z and Falnes, J (1996). "State-Space Modelling of a Vertical Cylinder in Heave," *Appl. Ocean Res.*, 17(5), 265−275.